



### RESEARCH ARTICLE

10.1002/2016WR018660

#### Key Points:

- Scale-dependent transfer functions can be used to evaluate scaling in fractured aquifers
- The method is inexpensive, able to sample statistical hydrogeological properties
- Single-porosity and dual-porosity formulations show different scaling behavior of selected variables

#### Supporting Information:

- Supporting Information S1

#### Correspondence to:

D. Pedretti,  
dpedretti@eos.ubc.ca

#### Citation:

Pedretti, D., A. Russian, X. Sanchez-Vila, and M. Dentz (2016), Scale dependence of the hydraulic properties of a fractured aquifer estimated using transfer functions, *Water Resour. Res.*, 52, 5008–5024, doi:10.1002/2016WR018660.

Received 22 JAN 2016

Accepted 21 MAY 2016

Accepted article online 26 MAY 2016

Published online 2 JUL 2016

## Scale dependence of the hydraulic properties of a fractured aquifer estimated using transfer functions

D. Pedretti<sup>1</sup>, A. Russian<sup>2</sup>, X. Sanchez-Vila<sup>3</sup>, and M. Dentz<sup>4</sup>

<sup>1</sup>Department of Earth, Ocean and Atmospheric Sciences, University of British Columbia, Vancouver, British Columbia, Canada, <sup>2</sup>Geosciences Montpellier, Université de Montpellier, Montpellier Cedex, France, <sup>3</sup>Hydrogeology Group (GHS, UPC-CSIC), Department of Civil and Environmental Engineering, Universitat Politècnica de Catalunya, Barcelona, Spain, <sup>4</sup>Hydrogeology Group (GHS, UPC-CSIC), Institute of Environmental Assessment and Water Research, Spanish National Research Council (IDAEA-CSIC), Barcelona, Spain

**Abstract** We present an investigation of the scale dependence of hydraulic parameters in fractured media based on the concept of transfer functions (TF). TF methods provide an inexpensive way to perform aquifer parameter estimation, as they relate the fluctuations of an observation time series (hydraulic head fluctuations) to an input function (aquifer recharge) in frequency domain. Fractured media are specially sensitive to this approach as hydraulic parameters are strongly scale-dependent, involving nonstationary statistical distributions. Our study is based on an extensive data set, involving up to 130 measurement points with periodic head measurements that in some cases extend for more than 30 years. For each point, we use a single-porosity and dual-continuum TF formulation to obtain a distribution of transmissivities and storativities in both mobile and immobile domains. Single-porosity TF estimates are compared with data obtained from the interpretation of over 60 hydraulic tests (slug and pumping tests). Results show that the TF is able to estimate the scale dependence of the hydraulic parameters, and it is consistent with the behavior of estimates from traditional hydraulic tests. In addition, the TF approach seems to provide an estimation of the system variance and the extension of the ergodic behavior of the aquifer (estimated in approximately 500 m in the analyzed aquifer). The scale dependence of transmissivity seems to be independent from the adopted formulation (single or dual-continuum), while storativity is more sensitive to the presence of multiple continua.

### 1. Introduction

Fractured aquifer systems have been receiving increasing attention in the recent years due to their strategic importance for drinking water supply and as a resource for agriculture and industrial activities. Correct hydraulic parametrization of fractured aquifers requires an integrated approach capable of effectively describing the impact of randomly distributed fractures and matrix hydraulic properties upon the temporally varying flow patterns described at different observation scales. A general review of these concepts, including characterization methods and modeling solutions for fractured media can be found for instance in Berkowitz [2002].

Hydraulic parameters, such as aquifer transmissivity ( $T$ ) and storativity ( $S$ ), are commonly estimated by model fitting of observed groundwater fluctuations associated with one or more external stresses (such as natural aquifer recharge or pumping). While most traditional estimation methods rely either on classical model curve fitting [e.g., Zech *et al.*, 2015] or else on inverse calibration approaches [e.g., Zhou *et al.*, 2014], recent applications have focused on transfer function (TF) estimation methods as a potential alternative method [e.g., Denic-Jukic and Jukic, 2003; Liao *et al.*, 2014; Pinault *et al.*, 2001; Trincherro *et al.*, 2011; Jimenez-Martinez *et al.*, 2013]. In TF methods, the aquifer is seen as an effective filter that transforms recharge signals into aquifer head or discharge fluctuations. From the initial formulations of TF methods [Gelhar, 1974], several alternative models based on stationary and nonstationary aquifer assumptions have blossomed [e.g., Zhang and Schilling, 2004; Schilling and Zhang, 2012]. As TF models are usually formulated in the frequency domain, they become particularly suited for the analysis of fractured media, where the hydraulic properties are conveniently represented using nonstationary statistical distributions [e.g., Barton and Larsen, 1985; Bonnet *et al.*, 2001; Berkowitz, 2002; Zhang and Li, 2005; Little and Bloomfield, 2010].

Fracture media as well as porous media display scale effect of estimated hydraulic parameters [e.g., *Brace*, 1980, 1984; *Clauser*, 1992]. This effect occurs since model outputs are sensitive to the support volume of the observations, the support scale of measurements and the adopted interpretation method [e.g., *Guimerá et al.*, 1995; *Sanchez-Vila et al.*, 1996; *Beckie*, 1996; *Guimerá and Carrera*, 2000; *Schulze-Makuch and Malik*, 2000; *Lai and Ren*, 2007]. For instance, in systems characterized by randomly distributed high-permeable fractures embedded into a low permeable matrix, there is a positive correlation between estimated  $T$  and the support scale of hydraulic tests [e.g., *Le Borgne et al.*, 2006]. This occurs since a large support scale generally corresponds to a larger probability of sampling high-conductive connected fractures, such that the average  $T$  increases with scale. When the support scale is of the order of or larger than the characteristic heterogeneity scale, estimated  $T$  values reach an asymptotic value [e.g., *Sanchez-Vila et al.*, 1996], which defines the scale of aquifer ergodicity. Scale dependence of  $S$  has been also reported in the literature and directly linked with aquifer heterogeneity and connectivity as well as the interpretation method used in the hydraulic test data analysis [e.g., *Meier et al.*, 1998; *Sanchez Vila et al.*, 1999].

*Jimenez-Martinez et al.* [2013] discuss the apparent scaling effects of  $T$  and  $S$  in a heterogeneous fractured aquifer in Ploemeur (Brittany, France). They compared estimations obtained from traditional hydraulic tests against those obtained from hydraulic responses analyzed by two single-porosity TF models, namely the Linear Model and an approximated Dupuit Model (DM) [*Gelhar*, 1974], both of which ignore the spatial dependency of observations related to the distance from the aquifer discharge point ( $x_L$ ). Compared to traditional hydraulic tests, these authors found that the TF-based approaches provided, on average, larger  $T$  and  $S$  estimates, combined with low-estimation variances, with a convergence of  $T$  at large scale toward the largest  $T$  estimates measured at smaller scales. Moreover, *Jimenez-Martinez et al.* [2013] obtained  $S$  estimates much larger than typical values associated with confined fractured aquifer. The authors explained this observation by indicating that the methods with low-support volume (flowmeter and pumping tests) tend to preferentially capture low-storativity features, which respond faster to hydraulic perturbations, while TF methods quantify processes at the basin scale, which may have a large overall storage.

The objective of this work is to provide insights on scale effects observed in the well-characterized fractured aquifer at the El Cabril Site, located in Southern Spain (Figure 1a), using single and multicontinuum DM formulations. We specifically focus on  $x_L$  as a key parameter to understand scale effects of estimated parameters obtained from TF models. The experimental database used in this work consists of more than 60 estimates of hydraulic properties obtained from model fitting of slug and pumping tests performed in several boreholes, sparsely located in the aquifer, and more than 130 head fluctuation time series collected during more than two decades in an equivalent number of boreholes.

The first goal of this analysis is to compare estimates of hydraulic parameters obtained from slug and pumping tests against those obtained from the scale-dependent, single-porosity DM of *Gelhar* [1974]. The objective is to evaluate if the scale effects upon estimated  $T$  and  $S$  values may be directly related to  $x_L$ , and therefore to analyze if TF methods are sensitive to the measurement and support scales, in a similar fashion as traditional testing approaches.

A second goal is to apply and discuss the results obtained by model fitting of a nonlocal dual-continuum TF formulation derived from the DM solution as reported in *Russian et al.* [2013]. Several investigations have shown that the anomalous behavior of flow and solute transport in fractured aquifers is sometimes better described and modeled using multicontinuum formulations [e.g., *Moench*, 1995; *Haggerty and Gorelick*, 1995; *McKenna et al.*, 2001]. Evidences of effective dual-porosity behavior of El Cabril aquifer were already observed by *Sanchez-Vila and Carrera* [2004], indicating that the system can be conceptualized as a medium that is composed of an effective fast-flow region (representing the fractures) overlapped to one or multiple low-permeability regions (representing the matrix), all regions exchanging water driven by head gradients. Emphasis is placed in this study toward the sensitivity of the solution to the different parameters involved in the conceptual model.

Initially, we introduce the study area in section 2, focusing on the key geological and hydrogeological aspects and in particular on the measured fracture index. In section 3, we present the estimates of transmissivity and storativity obtained through classical slug and pumping tests and in section 4 we focus on TF methods. Section 4 includes an introduction of the theoretical single and dual-porosity models, the

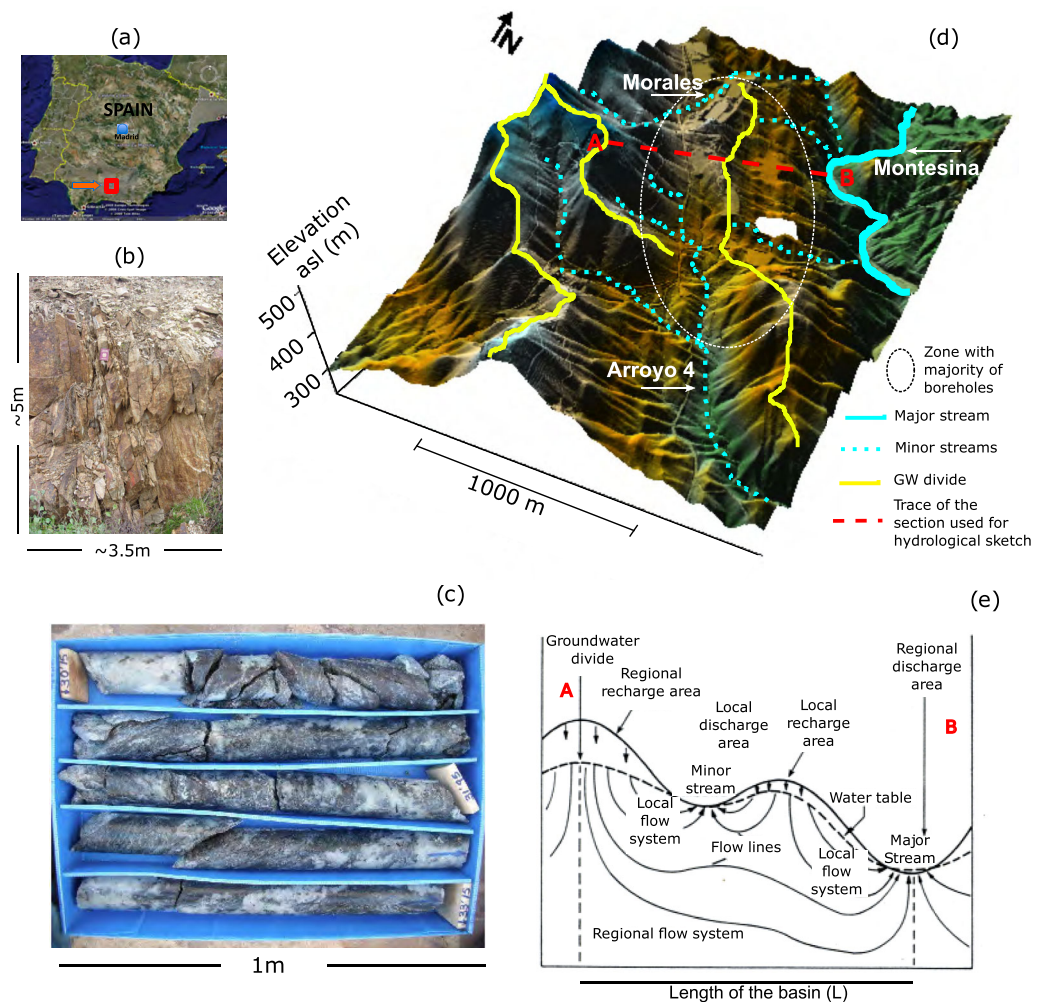


**Figure 1.** (a) geographical location of the El Cabril Site; (b) outcrop illustrating the intensity of rock fracturing in the site; (c) a representative drilling core box from one of the boreholes used to compute the RQD index; (d) the digital elevation model of the site, reporting the main surface hydrological patterns at the site ( $10^3$  m scale); (e) the conceptualization of the groundwater dynamics at the site, including regional and local flow paths.

derivation of the experimental TF and an illustrative example. The analysis and the discussion of the results are provided in section 5 and the conclusion in section 6.

## 2. Site Description

### 2.1. Key Geological and Hydrogeological Aspects

El Cabril Site is located in Southern Spain, Figure 1a, and hosts the Spanish repository for nuclear waste material of low and medium level activity. The fractured aquifer underneath the facility has been widely investigated in the past using multiple approaches, aiming to estimate effective hydraulic and transport properties to become an input in risk assessment exercises [e.g., BRGM, 1990; Carrera et al., 1993; Sanchez-Vila and Carrera, 1997; Meier et al., 1998; Sanchez-Vila and Carrera, 2004; Trincherro et al., 2008].

The geological nature of El Cabril aquifer is metamorphic. The main lithologies are biotitic gneisses and metaarkoses, which originated from sedimentary deposits and magmatic rocks. These materials suffered from several regional structural processes (including high-energy compressive Hercynian deformation), and more recent low-energy localized events. The combination of events resulted in tilting, faulting and an intense net of fractures, visible from several outcrops in the area (Figure 1b). The main orientation of the tilted structures is NW-SE, with fracture planes and sedimentary layers tilted up to  $90^\circ$  and directions  $60^\circ$ N

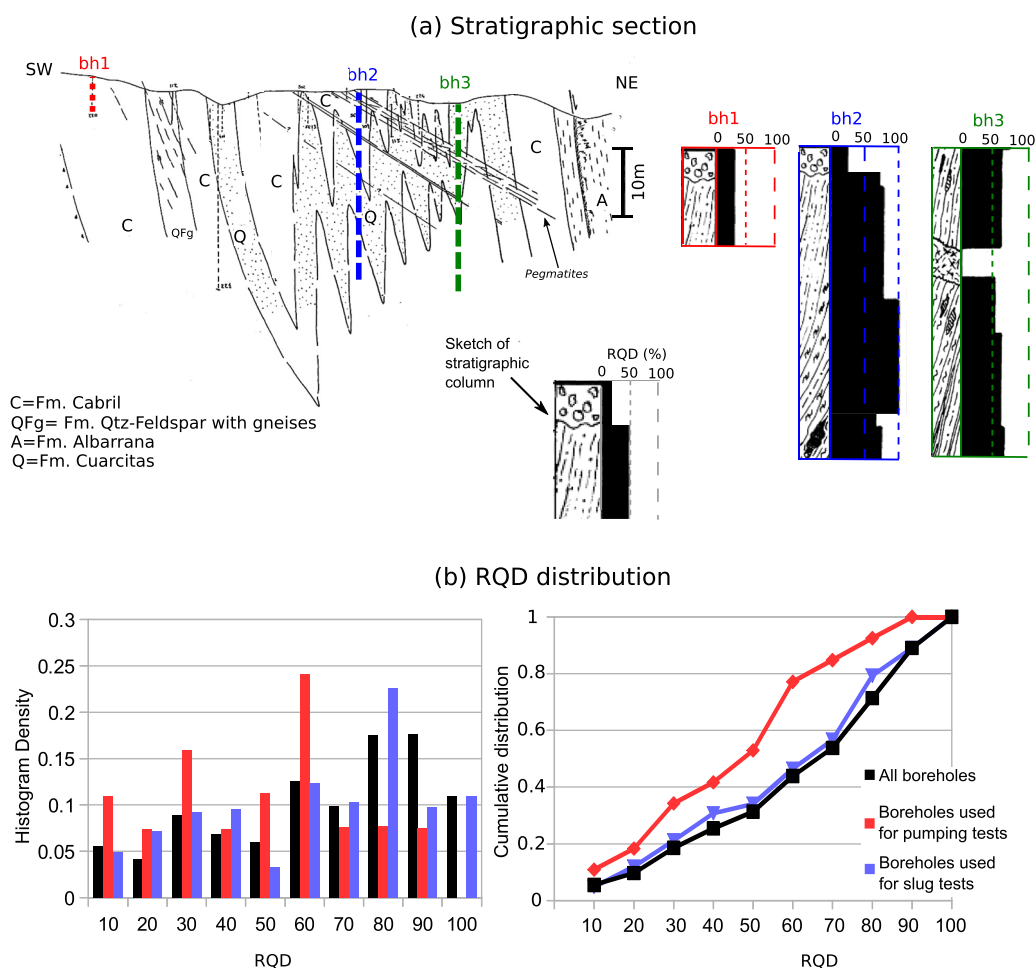


**Figure 2.** (a) Geological sketch of El Cabril (oriented NE-SW) and three representative stratigraphic columns with vertical distribution of the corresponding logs and the calculated RQD values; (b) frequency histogram and cumulative density of RQD at the El Cabril site. Black colors refer to the distribution obtained from all existing data; red and blue refer to distributions obtained from the subsample of boreholes used for pumping and slug tests, respectively.

to 90°N. A representative geological cross section, oriented perpendicular to the main direction of faulting, is illustrated in Figure 2a, showing the different formations, defined by geological criteria and genetic content of the local rocks. The main ones are called Fm *Cabril* (C), Fm *Cuarcitas* (Q), a formation composed of quartz and feldspar with gneisses (QFg), and Fm *Albarrana* (A).

Drilling cores from local boreholes and outcrops suggest that fracture spacing is very broad, ranging from  $10^{-3}$  to  $10^{-1}$  m (Figure 1b). Drilling cores exist for most of the boreholes. An example of these cores is shown in Figure 1c, where the lengths of intact (i.e., unfractured) core portions are well identified and used to compute the index of fracture intensity (rock quality designation, RQD), a relevant parameter in the analysis and addressed in the next section.

The presence of oriented fractures and the topography of the site control the average groundwater dynamics at the site. The morphology of the site is highly irregular, and the hydrological and hydrogeological patterns show a well-defined recharge zone located at high elevation and multiple local discharging locations at topographical lows (Figure 1d). Two minor streams (Morales and Arroyo 4) and a major stream (Montesina) are considered the major discharge feature at the subregional scale, as conceptually depicted in Figure 1e. Most of the boreholes analyzed in this work are located in the central valley and the crest of the intermediate groundwater divides.

The majority of the boreholes existing in the area were used as single-level piezometers to monitor the groundwater fluctuation. Of these, 138 boreholes were constantly monitored for several decades, reaching

in some cases 30 years. The sampling interval for the majority of the wells was either about 1 day or 15–30 days (supporting information), depending on the location. The depth of the piezometers varied between tens and hundreds of meters. A subset of these boreholes were also used to perform several hydraulic and tracer tests. From their analysis, it was concluded that the fracture orientation and intensity generate a strong anisotropy in aquifer hydraulic conductivity, with a major control on groundwater flow patterns. This was corroborated from the analysis of pumping tests and breakthrough curves (BTCs) measured during convergent flow tracer tests performed with different tracers and injecting at different locations in the aquifer, which suggested marked differences in responses displaying strong anisotropic effects [Sanchez-Vila and Carrera, 1997] and fracture connectivity [Trincheri et al., 2008]. Evidence of an effective dual-porosity hydraulic behavior of the aquifer can be inferred from the work of Sanchez-Vila and Carrera [2004], who illustrated that a nonlocal advection-dispersion formulation accounting for fracture-matrix mass exchange was able to fit observed BTCs during the tracer tests, while a single-porosity solution failed to reproduce similar observations.

## 2.2. Fracture Index

As discussed for instance by Jimenez-Martinez et al. [2013], the degree of fracturing of an aquifer can condition the flow patterns and eventually propagate to the estimated parameters. The quality and the integrity of the rock removed from the borehole can be described by the RQD Index, which measure the degree of fracturing of the core. RQD is defined from the proportion of the core with intact length larger than 0.1 m [Deere, 1963; Priest and Hudson, 1976]. To calculate this index, intact lengths from drilling boxes are summed up and expressed as a percentage of the total borehole length ( $B_L$ ), as:

$$RQD = \frac{100}{B_L} \sum_{i=1}^n z_i, \quad (1)$$

where  $z_i$  is the length of the  $i$ th rock fragment exceeding 0.1 m and  $n$  is the number of samples  $\geq 0.1$  m. The larger the RQD, the more intact (i.e., less fractured) the borehole log. Thus, RQD = 100% indicates an intact core (no significant fracturing observed). On the other limit, an RQD = 0 indicates the core is fully fractured into small pieces.

The vertical distribution of RQD in the aquifer was available from a few stratigraphic logs of boreholes reported during drilling operations. Some of these boreholes were also used later for hydraulic testing, allowing for performing a comparison between local degree of fracturing degree and estimated model parameters at different scales (those representative of the tests).

We analyzed the original stratigraphic logs of 76 boreholes (distributed all throughout the site), for a total length of approximately 4000 m of borehole scanlines. In each log, RQD was graphically reported alongside the corresponding stratigraphic column. An example is displayed in Figure 2a, showing three representative stratigraphic columns obtained from the data set. The black bars beside the vertical geological columns represent the frequency of fracture intensity with depth. The statistics of RQD values used in this work were inferred from the size of these bars (existing data are only graphical). Note that in this figure, the vertical scale of the columns is not consistent with the actual lengths of the boreholes but was adapted here for illustrative purposes. Their real vertical size of the columns is reported by the dotted line on top of the geological sketch, which also illustrates the position of the three columns in the aquifer. Figure 2a illustrates a few important aspects regarding the distribution of inferred fractures in the aquifer, and provides a general idea about the quality and limitation of the available information obtained from our data set.

The first borehole log analyzed (bh1) is shorter than the other two, and explores only the upper part of Fm C. Despite the presence of an upper recent alluvial material, the RQD reported was constant for the entire column, roughly corresponding to RQD = 40%. The second point (bh2) spans 40–50 m and is characterized by an initial low-RQD zone (associated with alluvial deposits), followed by a region with RQD = 75% and a subsequent region with RQD = 100%, again followed by a final zone with RQD = 75%. From the geological sketch, the area of RQD = 100% roughly corresponds to fm Q, while the portion with values of 75% are mostly associated to Fm C. In point bh3, the borehole still crosses multiple geological formations; however, RQD seems almost homogeneously distributed along the depth, with an average of 55–60% independent of the specific formation. An exception is found in an intermediate location where an elevated fracture intensity occurs with RQD = 0%. It is emphasized however that, on average, the majority of stratigraphic

logs are more similar to bh2 than to bh1 and bh3, which seems to suggest that in most parts of the aquifer the vertical distribution of RQD is heterogeneous and characterized by a sequence of high and low fracturing zones. The importance of this aspect will be clarified later, during the analysis of the estimated hydraulic parameters.

The statistical distribution of RQD from all 76 analyzed boreholes is reported in Figure 2b, in the form of frequency histograms (left) and cumulative density functions (cdfs) (right). It was found that the majority of the borehole logs analyzed display values of RQD > 50%, with highest frequency values located in the range 80–90%. However, about 35% of the total explored borehole scanlines show RQD < 50%. The red and blue lines indicate the subset of these boreholes which were used to perform slug and pumping tests in the 1990s (described below). It is noted here that the statistical distribution of RQD for the boreholes where slug tests were performed provide similar distribution as compared to the full population. This is not the case for the boreholes used for pumping tests where the distribution is shifted toward the left (low-RQD values), indicating a bias toward highly fractured zones in the development of pumping tests.

The analysis of the three-representative boreholes and the statistics of RQD at the scale of the catchment suggest some important geological aspects of this site. El Cabril aquifer does not systematically present a trend in fracturing index with depth, as observed at the aquifer investigated by *Jimenez-Martinez et al.* [2013]. RQD varies with depth in an unstructured random way. The comparison between bh2 and bh3 in Figure 2 suggests in addition that there is no clear correlation between RQD and the type of formations within this aquifer. This is consistent with the presence of postdepositional tectonic effects of the site, affecting all geological formations regardless of their genetic origin.

At the scale of the catchment, RQD is negatively skewed. The majority of the aquifer presents very few fractures and a generally intact (i.e., low fractured) matrix. This result is in line with past analyses made on this site and agrees with the general conclusions made on the regional hydraulic behavior of this aquifer, which is expected to behave as a low-permeable crystalline formation, in which a few highly conductive features carry the majority of water. This result is also consistent with common observations made on rock apertures [e.g., *Tsang and Tsang*, 1989]. Intuitively, one might expect that the aquifer permeability could be inversely correlated to RQD (i.e., permeability increasing with fracture intensity). Therefore, the permeability distribution at the scale of the catchment may be expected as positively skewed, with a larger amount of low-permeable zones and fewer high-permeable zones, consistent with typical observations on rock formations [e.g., *Gustafson and Fransson*, 2005]. It is finally noted that aquifer permeability may not directly correlate with 'static' indicators, such as RQD. Indeed, hydraulic properties are effective dynamic parameters and therefore require a dynamic solution to be properly estimated [e.g., *Le Borgne et al.*, 2006]. This is an essential point of this discussion, since it motivates the presence of scaling effects of estimated hydraulic parameters. The application of theoretical approaches that quantitatively relate RQD or similar geomechanical fracture indexes with rocks permeability [e.g., *Liu et al.*, 1999] need to be inspected carefully before being applied to estimate regional hydrodynamic behavior of fractured aquifers.

### 3. Hydraulic Parametrization From Slug and Pumping Tests

Several hydraulic tests were performed from the 1990s on to characterize the behavior of El Cabril using a suite of techniques. We focus here only on slug tests and pumping tests. In the former, head change is recorded as a function of time at the same well where an instantaneous stress is applied, while in the latter, the head change is observed both at the active well where continuous pumping is performed, and at a number of piezometers located nearby. The different support scale between the two types of tests (larger from pumping tests than for slug tests) results in scaling effects of estimated  $T$  and  $S$ , as reported by *Meier et al.* [1998].

Slug tests were interpreted under the assumption of 2-D radial flow in a homogeneous, single-porosity aquifer using the method of *Papadopoulos et al.* [1973]. The tests were performed in locations distributed across three of the different geological formations (Fms C, Qfg, and A). The results for estimated  $T$  and  $S$  in terms of cumulative frequencies from the existing 18 slug tests are reported in Figure 3. This same subset of boreholes was the one used to construct the histogram corresponding to the RQD index (Figure 2b).

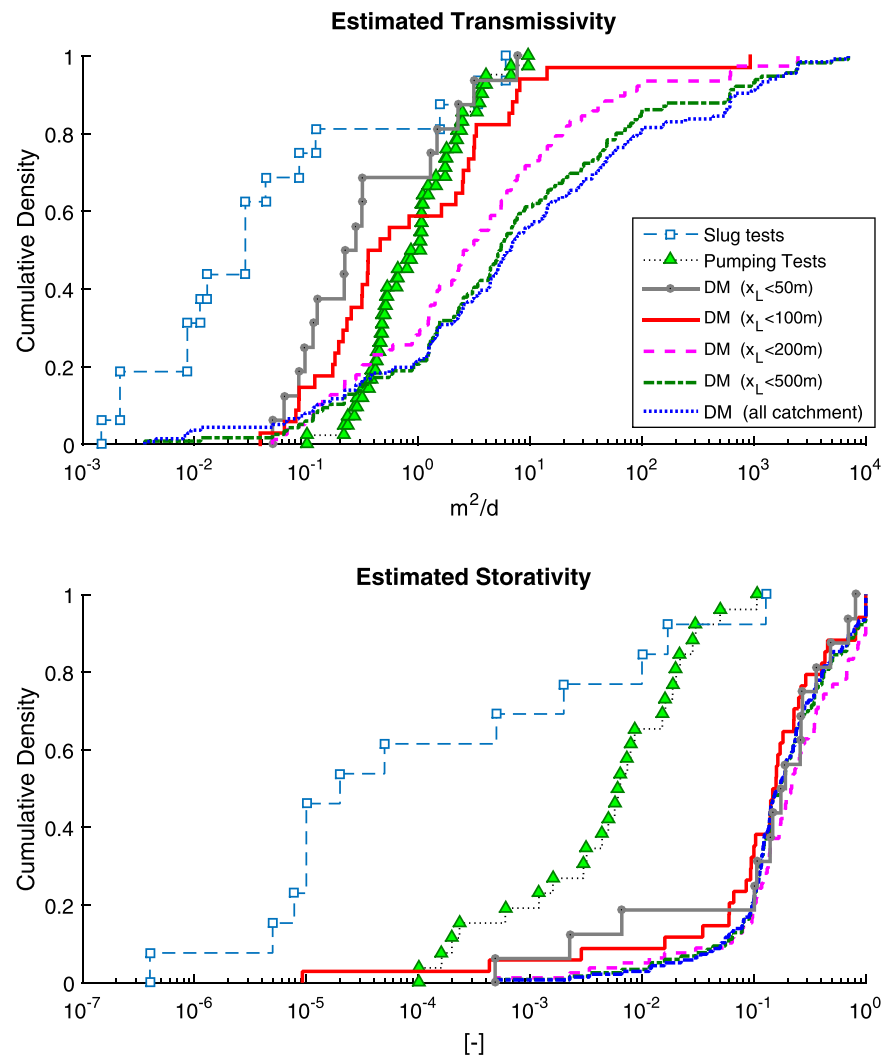


**Figure 3.** (top) Cumulative distributions of transmissivity ( $T$ , in  $m^2/d$ ) and (bottom) storativity ( $S$ , dimensionless) obtained from (squares) slug tests, (triangles) pumping tests, and from fitting of experimental TFs with the DM associated to boreholes located at (gray circles)  $x_L < 0.05$ , (red solid)  $x_L < 0.1$ , (pink dashed)  $x_L < 0.2$ , (green dash-dotted)  $x_L < 0.5$ , and (blue dotted) data from the whole catchment.

Two long-term pumping tests were performed in the early 1990s [e.g., BRGM, 1990]. The first one was made around pumping well S33. The drawdown curves from nine observation boreholes located nearby were interpreted for estimated  $T$  and  $S$  using the code MARIAJ [Carbonell and Carrera, 1992], which is based on a single-porosity solution. The original reports indicated that S33 was all drilled in Fm C, mainly composed by gneisses. No stratigraphic log (or RQD values) is available for S33. The piezometers were located into two different formations (Qfg and Q). According to field observations, piezometers drilled in Fm Q had a faster and larger response than those in Fm Qfg. A second long-term test implied pumping at well S401, located far from S33 but also drilled in Fm C. Drawdown curves from seven piezometers located in the proximity of the well were monitored and used to estimate  $T$  and  $S$  using the same methodology as for the previous test. Boreholes were drilled in three different formations (Fms C, Q, and QFg).

Several short-term pumping tests were also performed in other boreholes located all throughout the site. A similar single-porosity modeling approach was used for the interpretation, although no specific details regarding the geological formations explored by these tests were available. In total, the number of estimated parameters from short-term and long-term pumping tests was 42 estimates of  $T$  and 30 estimates of  $S$ . These results are plotted in Figure 3 in the form of cumulative frequencies.

Comparing estimated values from slug and pumping tests in Figure 3, it can be observed that the estimated values display the typical scaling effect associated with the different support scales for the corresponding hydraulic tests. Estimates from slug tests show lower average  $T$  and  $S$  values and a higher variability than those coming from pumping tests.  $T$  estimates range over four orders of magnitude for slug tests, being around two orders for pumping tests. Regarding the estimated  $S$  values, the variability ranges over more than five orders of magnitude for slug tests and about three for pumping tests. It is interesting to note that the resulting estimates of  $S$  display a range of values spanning from typical values for confined aquifers ( $S \in [10^{-4}, 10^{-5}]$ ) to values representative of unconfined aquifers ( $S \approx 10^{-1}$ ).

Estimated  $T$  and  $S$  values reveal that the aquifer is not only highly heterogeneous, but also characterized by a different effective pressure status depending on the test locations. The pressure status depends directly on the number of confined/unconfined units and potentially by the fracture intensity from the boreholes where these tests were performed. Figure 2b shows that the cumulative frequency of RQD for the boreholes used in the pumping tests (red lines/bars) is significantly different than that from slug tests (blue lines/bars). Specifically, RQD corresponding to the former display a larger amount of low-RQD values as compared to that corresponding to slug tests. In particular, no boreholes with  $RQD > 90\%$  were reported in the subset corresponding to locations where pumping tests were performed.

The statistical difference in RQD between both populations may contribute to explain the differences observed in Figure 3, as well as the associated scaling effects between the estimates for the two test types. The effective support scale of each hydraulic test depends on the amount of heterogeneity which is sampled by the specific test. Hence, hydraulic tests performed in low-RQD zones result in relatively larger  $T$  estimates with lower variability than tests performed in areas with higher RQD. Low-RQD values mean short lateral continuity of fractures, which can be associated with a lower hydraulic connectivity of the system and quasi homogeneous hydraulic properties around each borehole. Contrarily, a high fracture intensity can determine a vertical continuity between the ground surface and the subsurface. This may explain why larger estimated  $S$  values are reported for pumping tests as compared to those for slug tests.

#### 4. Parameter Estimation Using Transfer-Function-Based Methods

The transfer function is generally conveniently defined in frequency domain as the ration of the power of the spectrum of the aquifer response (e.g., hydraulic head fluctuation at a piezometer) to an input signal (e.g., recharge,  $r$  [m]), such as:

$$TF = \left| \frac{h(x, \omega)}{r(\omega)} \right|^2, \tag{2}$$

where  $h(x, \omega)$  is the hydraulic head [m] for given position  $x$  [m] and frequency  $\omega$  [1/d]. Parameter estimation using TF approaches is based on model fitting of closed-form analytical TF solutions to match experimental TFs. Estimated parameters directly depend on the selected formulation and the type of boundary conditions (BCs) applied at the outflow boundary of the aquifer, and the type of flow formulation (e.g., single-porosity or multiporosity domain). The reader is referred to *Russian et al.* [2013] for an exhaustive review of these concepts. In the following, we present the transfer functions for the single and dual domain DMs, which we adopted for the analysis of the El Cabril site.

##### 4.1. Dupuit Model

The first model adopted in this work is the single-porosity DM by *Gelhar* [1974]. The DM describes flow in the aquifer based on the linearized Dupuit-Forchheimer model [e.g., *Bear*, 1972]. The model takes the form of:

$$S \frac{\partial h(x, t)}{\partial t} = T \frac{\partial^2 h(x, t)}{\partial x^2} + r'(t), \tag{3}$$

where  $S$  is the storage coefficient [-],  $t$  is time [d],  $T$  is the transmissivity [ $m^2/d$ ], and  $r'(t)$  is the aquifer recharge rate per unit surface [m/d], which is assumed to be homogeneous. For the initial condition ( $h_0=0$ ) and a Dirichlet BC at the outfall, the TF reads as [*Russian et al.*, 2013]:

$$TF_{DM} = \frac{1}{\omega^2 S^2} \left| 1 - \frac{\cosh[\sqrt{i\omega\tau}(1-x_L/L)]}{\cosh(\sqrt{i\omega\tau})} \right|^2, \tag{4}$$

where  $i = \sqrt{-1}$  is the imaginary unit and  $\tau = L^2 S / T$  is the aquifer response time [d]. The inverse of the aquifer response time is named aquifer response rate ( $\omega_L$ ) [Erskine and Papaioannou, 1997] and defines one characteristic frequency of the model, such as  $\omega_L = \tau^{-1}$ .

As pointed out in Russian et al. [2013],  $x_L$  identifies another characteristic frequency given by the mean diffusion time from the observation point to the discharge point, such as  $\omega_x = T / (x_L^2 S)$ . These two characteristic frequencies determine the scaling behavior of the TF:

1. for  $\omega \ll \omega_L$  the TF is flat, which means that long-time components in the recharge spectrum, with frequency lower than the aquifer response rate are not smoothed by the aquifer;
2. for  $\omega \gg \omega_x$  the characteristic scaling of TF for the DM is  $TF_{DM} \propto \omega^{-2}$ ;
3. for  $\omega_L \ll \omega \ll \omega_x$  and if  $x_L \ll L$ , a third regime develops, where  $TF_{DM} \propto \omega^{-1}$ .

We refer the reader to Russian et al. [2013] for details. The distance from the domain boundaries, here from the discharge boundary defines the sampling scale of aquifer heterogeneity that influences the hydraulic head response to the recharge signal. For a well located close to the outfall or the watershed, the sampled heterogeneity scales are of the order of or smaller than the distance to the respective boundary.

#### 4.2. Dual-Continuum Nonlocal Dupuit Model (DC)

The second model considered is the dual-continuum (DC) nonlocal TF model developed in Russian et al. [2013]. The model mimics the presence of nonequilibrium effects associated with water storage in multiple low-permeable zones within the aquifer using an effective formulation and allows for a broader range of possible scalings of the TF with frequency. The selection of the DC model is based on dual-continuum behaviors observed for tracer tests at the El Cabril site.

In the dual-continuum approach, the aquifer is conceptually represented by two zones or “domains”: a mobile domain ( $m$ ), representing the fractures, and an immobile ( $im$ ) domain, representing the matrix. Water moves mainly through the highly conductive fractures according to the hydraulic gradient, and may be transferred into the matrix where it is stored for a certain time. The transfer rates between the mobile and immobile domains are encoded in a memory function [Carrera et al., 1998; Russian et al., 2013] as outlined below. The evolution of the hydraulic head in the mobile region ( $h_m$ ) is described by the nonlocal Dupuit equation [Russian et al., 2013]:

$$S_m \frac{\partial h_m(x, t)}{\partial t} = T_m \frac{\partial^2 h_m(x, t)}{\partial x^2} + r'(t) + F_{im}(x, t), \tag{5}$$

where  $F_{im}$  is a source/sink term defined as:

$$F_{im}(x, t) = S_{im} \frac{\partial}{\partial t} \int_0^t g(t-t') h_m(x, t) dt', \tag{6}$$

where  $g(t)$  is the memory function defined below. For Dirichlet BCs at the outfall, the TF reads as [see equation (C2) in Russian et al., 2013]:

$$TF_{DC}(x_L, \omega) = \frac{1}{\omega^2 [S_m + S_{im}g(\omega)]^2} \left| 1 - \frac{\cosh[\sqrt{i\omega\tau_e(\omega)}(1-x_L/L)]}{\cosh[\sqrt{i\omega\tau_e(\omega)}]} \right|^2, \tag{7}$$

where  $S_m$  and  $S_{im}$  are the storage coefficients of the mobile and immobile zones, respectively and  $\tau_e(\omega) = L^2 [S_m + S_{im}g(\omega)] / T_m$ . The response time of the mobile domain is given by  $\tau_m = L^2 S_m / T_m$ . The memory function  $g(\omega)$  is defined in frequency domain as:

$$g(\omega) = \frac{1}{\sqrt{i\omega\tau_{im}}} \tanh \sqrt{i\omega\tau_{im}}, \tag{8}$$

where  $\tau_{im}$  is the relaxation time of the immobile zone.

The DC model is defined in terms of four parameters (transmissivity and storage coefficient of the mobile continuum, the storage coefficient and the relaxation time of the immobile continuum). Note that the

formulations for the local and nonlocal DM are very similar; actually, (7) tends to (4) as  $S_{img}(\omega) \rightarrow 0$ , which occurs when equilibrium is reached, this means for  $\omega \ll \tau_{im}^{-1}$ . To observe an impact of the immobile zone on the aquifer dynamics, the two relaxation time scales  $\tau_m$  and  $\tau_{im}$  must be clearly separated. This can be measured by the dimensionless “activation number”  $A_c$  defined as:

$$A_c = \left( \frac{S_m}{S_{im}} \right)^2. \tag{9}$$

If the activation number is  $A_c < 1$  the system “notices” an impact of the immobile zone. The smaller  $A_c$ , the larger the relevance of the nonlocal effects on the shape of TFs.

### 4.3. Derivation of Experimental Transfer Functions and Fitting Methodology

We computed experimental transfer functions ( $TF_{EXP}$ ) from head fluctuation time series obtained from 136 boreholes existing in the site. We used continuous recordings from different time intervals, which presented a few gaps that were filled by linear interpolation. The frequency of the measurements is constant for each piezometer, but varies from point to point (supporting information). We distinguished between two clusters of data, those with measurement intervals of about 15–30 days, and those with measurement intervals below or equal 1 day.

$TF_{EXP}$  is calculated as the ratio between the power-spectral density of spatially variable observed head fluctuations ( $PSD_h$ ) and the power-spectral density of the aquifer recharge ( $PSD_r$ ), as:

$$TF_{EXP}(\omega) = \frac{PSD_h(\omega)}{PSD_r(\omega)}. \tag{10}$$

No specific recharge analysis has been performed on this site, thus we take it homogeneously distributed in the domain, which is a reasonable approximation for small basin. To account for the high evaporation rates existing in the site (located in southern Spain), recharge is estimated as half the total precipitation. Hourly rainfall time series were collected at a meteorological station located in the basin. Runoff is assumed negligible.  $PSD_h$  and  $PSD_r$  are computed using the MATLAB native function “periodogram.m,” which adopts a nonparametric approach under the assumption of a wide-sense stationary random process and using discrete Fourier transform (DFT). No regularization approach was used to filter high-frequency signals, in order to minimize artificial spurious effects that could bias the parameter estimations.

The relative distance of each borehole from the discharge location ( $x_L$ ) is used as an entry parameter in the models. Using a simple GIS-based calculation,  $x_L$  was obtained by computing the minimum Cartesian distance from each borehole to the three main streams identified in the catchment (Montesina, Morales, Arroyo 4). Of the 136 boreholes used in this analysis,

1. 16 boreholes are located at  $x_L < 50$  m,
2. 34 boreholes are located at  $x_L < 100$  m,
3. 76 boreholes are located at  $x_L < 200$  m,
4. 116 boreholes are located at  $x_L < 500$  m.

As a working assumption, the catchment width is assumed to be constant for all boreholes and equal to  $L = 1000$  m (similar to maximum size of the three subcatchments). We performed a sensitivity analysis using a specific  $L$  for each borehole, based on the size of the individual catchment, but obtained no remarkable difference compare with the results using a constant  $L$  (supporting information). As such, the results shown hereafter refer to a constant  $L$  value.

For each borehole, the TF for the DM, equation (4), and DC model, equation (7), were fitted to experimental TFs using a nonlinear least squares fit (MATLAB native function “lsqcurvefit.m”). The procedure is based on the minimization of an objective function, imposing a range of values and an initial estimation. The quality of the fitting exercise, measured through the regression coefficient  $R^2$ , was generally good (supporting information).

### 4.4. Representative Example

Figure 4 illustrates a representative example of experimental TFs. The top figure shows the head fluctuation in one of the boreholes, with average reading interval of 1 day, and in the middle the daily rainfall time

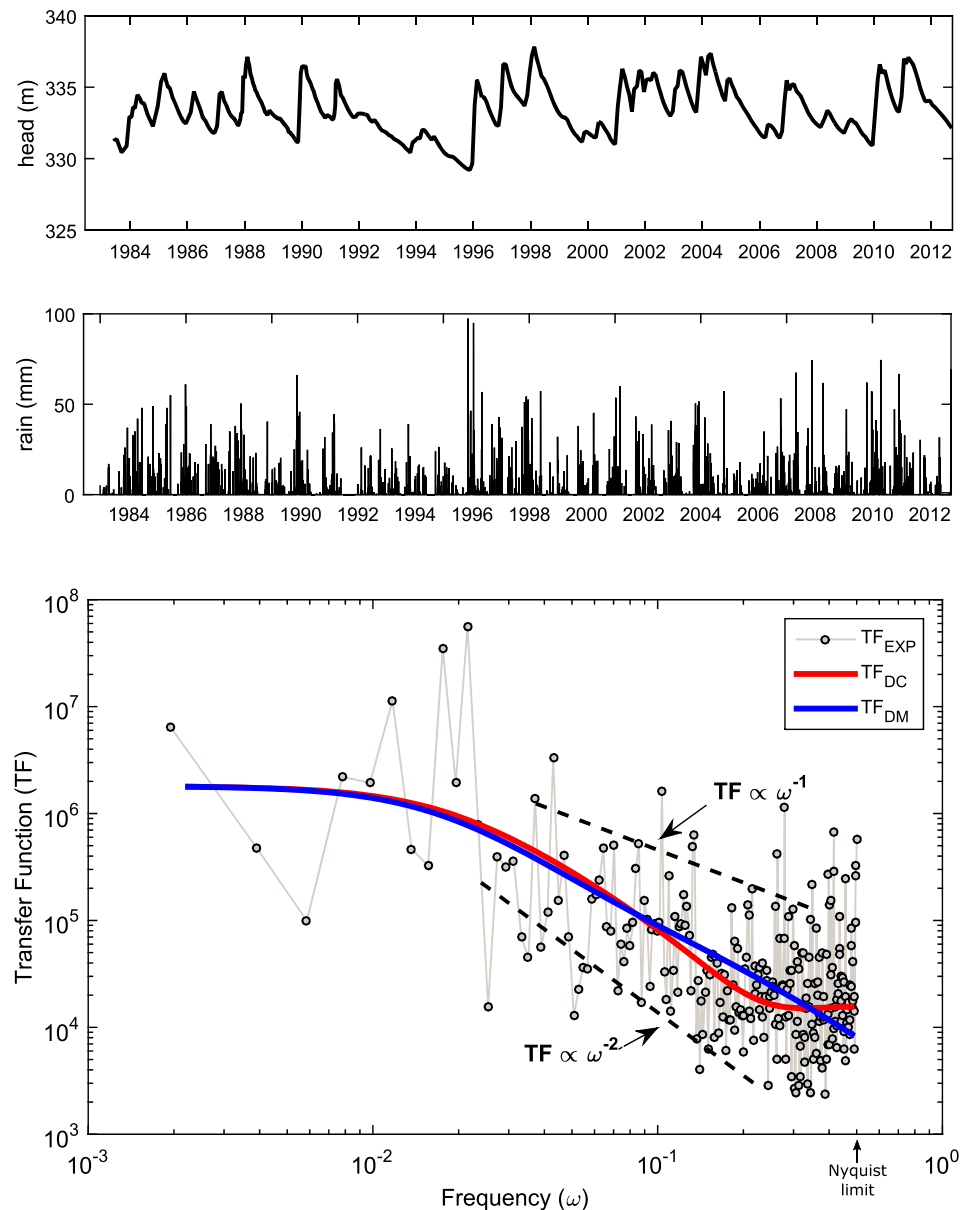


**Figure 4.** From top to bottom, a representative example of the hydrograph from one selected borehole, the rainfall time series and the resulting experimental transfer function ( $TF_{EXP}$ ), with the fitted models (DM = single-porosity, scale-dependent DM; DC = dual-continuum version of the DM).

series. At the bottom, the dotted gray line represents the calculated experimental TFs for this borehole, which is overlapped by the two fitted TF models (DC model in red and DM in blue). Two additional lines, scaling as  $TF \propto \omega^{-1}$  and  $TF \propto \omega^{-2}$ , are shown for illustrative purposes. The plot is reported in double log scales, which helps to infer the characteristic power-law distributions of the data.

Due to the noise, the characteristic shapes of theoretical TFs are only partially visible from the experimental TFs. At low frequencies, TFs tend to be flat, reflecting long-term hydraulic relationships (e.g., seasonal recharge processes). The lowest frequency corresponds to  $\omega = 1/365 \text{ d}^{-1}$ . Around  $\omega = 0.02$ , the experimental data seem to decrease at a rate  $\omega^{-1} < TF < \omega^{-2}$ , although the exact value is difficult to infer. For this specific data set, the maximum frequency is  $\omega_N = 0.5 \text{ d}^{-1}$ , where  $\omega_N = 1/(2\Delta t)$  is the Nyquist limit and  $\Delta t = 1 \text{ d}$ .

The two TF models displayed in Figure 4 fit the data set and help identifying the critical features from these data, including the inflection points. The first inflection point is found between low and mid frequencies

( $\omega \approx 0.02$ ) and corresponds to the characteristic response time of the mobile portion of the system ( $\tau$  and  $\tau_m$ , respectively, for the DM and DC models). We highlight that the scaling of this point is found at very similar frequencies for both DC and DM, suggesting that the scaling of  $T$ ,  $S$  and  $T_m$ ,  $S_m$  may also be similar.

Both models tend to scale as  $TF = \omega^{-2}$  at higher frequencies, although DC seems to reach this behavior earlier than DM. The reason is linked to the memory function term in the DC model, which generates a second inflection point occurring at high frequencies. The shape of the DC model is very similar to those predicted by the models by *Molénat et al.* [1999] and *Trincherò et al.* [2011]. The former describes the effective discharge of a basin as a combination of a fast hydrologic component such as lateral flow in the unsaturated zone and/or overland flow, and slow flow such as groundwater aquifer discharge. The latter combines the main groundwater flow to a more rapid component due to presence of highly-connected preferential flow channels. In our data sets, this means that the model is sensitive to the effects of short-term recharge processes and heterogeneity occurring at El Cabril. The DM is not able to reproduce these short-term processes, being incapable to reproduce this final scaling in the curve.

The behavior of experimental and theoretical curves shown in this specific example is qualitatively similar to the general behavior of the entire analyzed data set. However, the exact scaling of the best-fitting models varies from borehole to borehole, and consequently the resulting characteristic times ( $\tau$ ,  $\tau_m$ , and  $\tau_{im}$ ) and estimated parameters also significantly fluctuate at the scale of the catchment. This reveals important aspects related to scaling effects in estimated parameters, and the role of aquifer heterogeneity at El Cabril, which is the key result for our work. These points are analyzed and discussed in the next section.

It is ultimately highlighted that the high noise and the finite sampling frequencies may bias the estimation of this second inflection point. This requires attention when inferring behavior of the short-term recharge effects for a limited data set, and can be seen as a potential limitation of our analysis. A sensitivity analysis was run to quantify the impact of the different sampling frequencies, comparing the spatial dependence of parameters calculated exclusively from more complete and extended time series (having Nyquist limit  $N_f > 0.1$ ) against the results from the entire data set (which include extended and limited time series). The results of this sensitivity analysis (supporting information) seem to suggest that the finite sampling frequencies may have only a moderate impact on the estimated parameters and in particular on the scaling effects. Thus, the presence of high noise and the finite sampling frequencies do not affect our main conclusion on parameter estimation and scale effects.

## 5. Analysis and Discussion

### 5.1. Single-Porosity Models—Scale Dependence of Hydraulic Parameters Estimates

The resulting parameters obtained from TF-model fitting of the experimental data set are reported in Figure 3. To emphasize the impact of scaling effect, we report the statistical distributions of each parameter (in the form of cdfs), obtained from the ensemble of boreholes located within specific  $x_L$  thresholds. This is done such that each cdf integrates the impact of different heterogeneity scales on the hydraulic parameters.

We compare the estimates of  $T$  and  $S$  obtained with the TF of single-porosity DM for different  $x_L$  and the ones obtained from slug and pumping tests.

Figure 3 (top) illustrates the cdfs of  $T$  estimated with the different methods. For the cdfs of  $T$  corresponding to boreholes found at  $x_L < 100$  m, the mean values are smaller than those estimated from the full population of pumping tests, while the degrees of variability are comparable. As  $x_L$  increases, both the mean and variance of estimated  $T$  also increase, reaching a maximum when the boreholes from the entire catchment are considered ( $x_L = L$ ). By accounting for  $x_L$ , the TF method generates scaling effects of estimated  $T$  similar to those observed from traditional testing approaches. The distance  $x_L$  can be interpreted as the support scale of the scale-dependent TF model. Indeed, when the support scale is comparable with that of the pumping tests, the average  $T$  estimates are similar, suggesting that TF may embed the same average amount of information on aquifer transmissivity as traditional hydraulic testing approaches. This behavior is explained using similar arguments as *Le Borgne et al.* [2006]: when  $x_L$  is small compared to the scale of the catchment, the support scale of the TF is limited, a smaller number of fractures is sampled and the resulting average  $T$  is low; when  $x_L$  is large, the scale of the observation increases, the number of high-permeable zones increases and the average of the estimated  $T$  values grows.

Note that, as the scale of observation increases, the relative variability of  $T$  also increases, eventually becoming comparable with that of slug tests. This behavior, which seems to contradict the evidences by *Jimenez-Martinez et al.* [2013], must be related to the distribution of fractures in the aquifer. Similar to RQD for slug tests, the distribution of fractures in the aquifer is much broader than that of pumping tests. Hence, the relative variability in  $T$  estimates cannot be directly compared with that corresponding to pumping tests, since the effective support scale of TFs and pumping tests is biased by a different geological background where the tests were performed.

For small support scales, the relative variability of  $T$  from slug tests is much larger than that from TFs. This is explained considering that slug tests provide a local estimation of  $T$ , which depends on the specific area of influence where the stress is locally applied. It is also likely that slug tests tend to better sample the behavior of confined formations, which also has a quicker elastic response than unconfined formations. Therefore, slug test estimates become sensitive to the presence of small-scale heterogeneity in those formations. On the other hand, TF provides an integrated vertically averaged  $T$  value over the entire thickness of the aquifer explored by the boreholes, in which multiple formations and fractured are sampled. Most of the boreholes in this aquifer display a vertical distribution of RQD similar to that of bh2 in Figure 2 and each one samples multiple fractured zones, rather than displaying a homogeneous distribution. In addition, it is also reminded that the majority of head fluctuations is monitored through single-level piezometers and therefore the response of the aquifer to surface recharge is also vertically averaged.

The behavior of  $T$  is consistent with the resulting behavior of storativity  $S$  illustrated in the bottom panel of Figure 3. For small  $x_L$ , the smallest estimated  $S$  values are comparable with the largest values estimated from slug tests, whose relative variance is larger than the one estimated by TF. As  $x_L$  grows, the relative variance of the TF data is reduced and the estimated  $S$  scale at much larger average values than those from slug and pumping tests. As the scale of observation grows, the system becomes effectively equivalent to an unconfined formation. The weak dependency of the storativity with  $x_L$  agrees with the hypothesis of vertical communication induced by the fracturing intensity of the system. Fractures tend to facilitate communication between confined and unconfined formations in the aquifer. The impact of fractures grows with the sampling scales, since the observed fluctuation integrates a larger number of fractures at the observation points departs from the discharge point.

We observed no significant changes in the distribution of  $T$  between  $x_L < 500$  m and the full data set. This may indicate that ergodic conditions are reached at 500 m. This distance is shorter than the system's dimension but larger than the typical sampling scale of pumping tests. There are important practical implications associated with this finding. First, from a stochastic modeling perspective, it indicates that  $T$  may be simulated as a stationary field for domains larger than 500 m, while at shorter distance  $T$  can be considered as a nonstationary field. Second, TF methods are less expensive than traditional hydraulic tests and therefore may gain importance to quickly estimate ergodic scales. Indeed, TF statistics are obtained from a distribution of piezometers in the site that do not need to be characterized using expensive hydraulic tests. Note that hydraulic heads could be monitored over time using automatic data loggers, and thus be virtually costs-free (excluding initial capital costs and maintenance operations).

We may conclude that a critical analysis of the distribution of geological features in the aquifers and the actual position of observation points in the aquifer is fundamental to correctly predict scaling effects in heterogeneous fractured formations. Most of the apparent contradictions between our analysis and those reported by *Jimenez-Martinez et al.* [2013] stem from both the different geological and lithological nature of the explored aquifers and the use of a different interpretation model, specifically related to the explicit spatial dependency of the observation point simulated by the DM.

### 5.2. Comparison Between Single-Porosity and Dual-Continuum Formulations

We now compare the parameters estimated using the single domain DM against those obtained from model fitting of the DC model described in section 4.2. The estimated hydraulic parameters are reported in Figure 5, in the form of cdfs. Transmissivity and storativity of the mobile domain ( $T_m$ ,  $S_m$ ) are plotted along with  $T$  and  $S$  from the single-domain model, which are equivalent when the impact of immobile zone is not influencing the results (i.e.,  $A_c < 1$ ). The results suggest that scale-dependent effects are still observed for dual-domain estimates, although the estimates of both transmissivity and storativity are different for the single and dual-domain TFs.

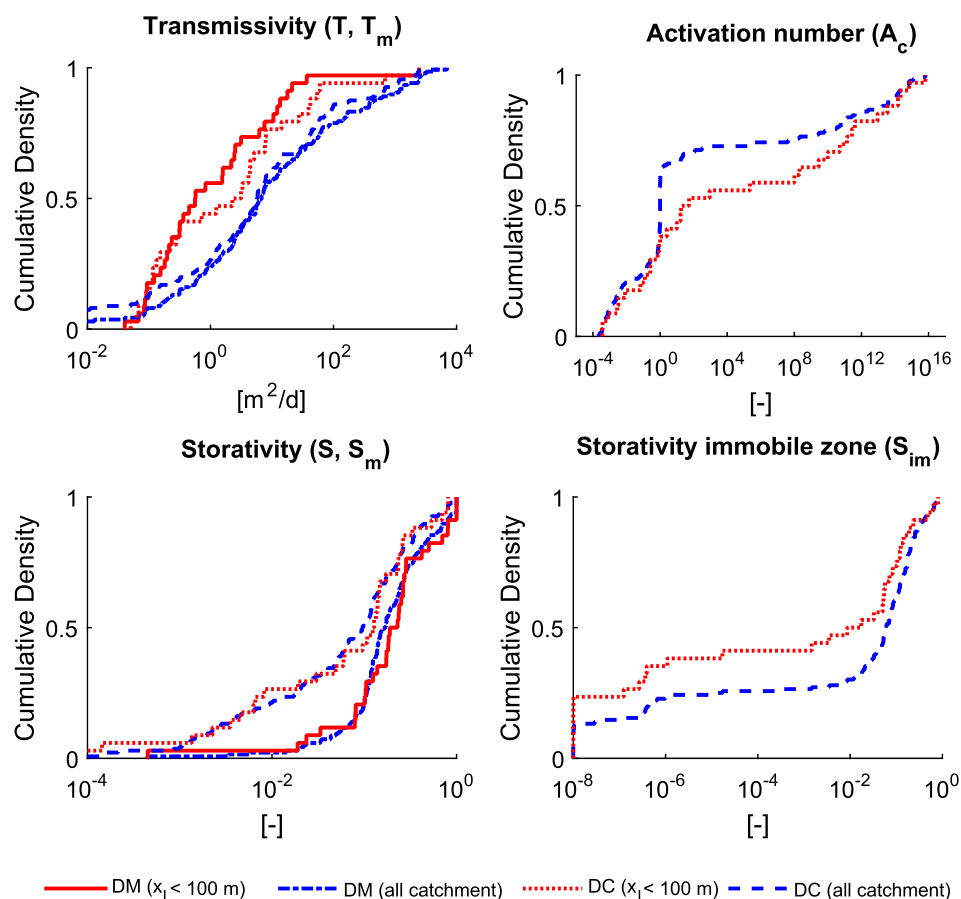


**Figure 5.** Cumulative distributions of (top left) transmissivities, (top right) activation number  $A_c$ , (bottom) storativity. Estimates from the DM are (red solid) for  $x_L < 100$  m and (blue dash-dotted) for the all the catchment. Estimates from the nonlocal DM (DC) are (red dotted) for  $x_L < 100$  m and (blue dashed) for the whole catchment.

Regarding the transmissivity, we found a difference in the cdfs for  $x_L < 100$  m depending on the adopted formulation. As the sampling scale increases, the difference in cdfs is minimized. This result seems consistent with the potentially strong control of fractures, connectivity, and heterogeneity on the flow dynamics at short distances between observation and discharge point. The resulting “anomalous behavior” of aquifer properties (which can be effectively upscaled using nonlocal models, such as the dual-continuum formulation) occurs when the scale of observation is lower than or comparable to the characteristic scale of heterogeneity. As the sampling scale increases, the aquifer becomes statistically homogeneous and apparent nonlocal effects on flow dynamics disappear, which is similar to the homogenization of solute transport in heterogeneous media as the scale sampled by the solute increases [e.g., Zinn and Harvey, 2003; Dentz et al., 2004; Pedretti et al., 2014].

The estimates of storativity are much more sensitive to the model choice than transmissivity. At any scale,  $S_m$  is generally lower than  $S$ , while  $S_{im}$  tends to increase as the sampling scale increases. It is observed, for instance, that approximately 50% of the fitted boreholes found at  $x_L < 100$  m display  $S_{im} > 10^{-2}$ , while the percentage increases to about 75% when the entire catchment is explored. Consistently,  $A_c \approx 1$  for about 40% of the fitted boreholes at  $x_L < 100$  m, while this percentage increases to more than 60% when the entire catchment is explored. This suggests that the significance of the immobile domain grows as the scale of domain increases.

The larger scale dependence of the storativity in the dual domain is due to the storage capacity represented by the immobile domain through  $S_{im}$ . This component is not present in single domain models, where all the storage capacity is lumped together into a single  $S$  value. It is likely that, at larger sampling scales, the behavior of the El Cabil aquifer superimposes a regional component, controlled by the mobile domain, and

a local one, controlled by preferential zones and small-scale fractures. Surface recharge controls the vertical oscillation of the aquifer, relevant only in unconfined aquifers. Consistent with what is discussed in the previous section for single domain models, the effective unsaturated behavior of the system may be controlled by the number of fractures that generate communication between confined and unconfined units. This number grows with the scale of the observations. At short observation distances, the impact of vertical fractures is less evident, explaining why the system is less sensitive to short-term recharge pulses.

We highlight, however, that at short observation distances the influence of both regional recharge components and short-term local components may also somewhat overlap, resulting in a mixed behavior on the TF which cannot be well fitted by nonlocal models. While the sensitivity analysis seems to suggest that the impact of higher sampling frequency does not qualitatively affect our conclusions (supporting information), we speculate that a very refined time discretization (e.g., order of minutes) could result in different tailing for experimental TFs at short-distance boreholes. This could be an indicator to discriminate between single and dual-continuum models at small  $x_L$ . No information is nonetheless available so far to corroborate this hypothesis.

We therefore conclude that transmissivities are rather insensitive to single or dual-domain interpretations of the data, since in both models water transmission is mainly occurring through the mobile fracture continuum. The dual-continuum model does not consider transmission in the immobile matrix continuum, which provides a storage volume. Thus, naturally, the storage capacities estimated for the single domain model and the mobile storage capacity are quite different. Therefore, it is likely that the general response of aquifer to recharge effects, which is controlled by the hydraulic diffusivity of the system, could be affected by the presence of effective low-permeable zones which may affect the transformation of recharge signals into head fluctuations. However, our analysis suggests that care must be taken when inferring general conclusions based on dual-continuum models if the sampling frequency is limited, since the impact of immobile zones may not be clearly observed.

## 6. Summary and Conclusions

We present an analysis of the scale dependence of hydraulic parameters (transmissivity and storage capacity) based on a transfer function analysis. The transfer function approach considers the aquifer as linear filter, which can be characterized by comparison of the power spectra of the input signals (aquifer recharge) and output signals (hydraulic head fluctuation). Its dependence on frequency allows to infer information on the hydraulic aquifer properties based on a physical process model, which here is given by single and dual-domain Dupuit aquifer models.

Unlike other approaches, we consider solutions to these models that explicitly account for the distance between the location of the observation wells and the discharge boundary ( $x_L$ ). This allows for a scale-dependent interpretation of the response data from boreholes at different locations, and thus to associate the estimated hydraulic parameters with a given support or sampling scale of the TF solution. Thus, the estimation of transmissivity and storage capacity is based on analytical solutions for transfer functions that are explicitly dependent on the distance to the recharge boundary.

We adopt the scale-dependent TF approach to analyze the El Cabril aquifer, which is a well-characterized aquifer in Southern Spain. We first evaluate the data in view of a scale dependence of transmissivity and storage capacity for the single domain model and compare the results to estimates from slug and pumping test, which sample different heterogeneity scales. We find that:

1. The estimates for transmissivity show pronounced dependence on  $x_L$  and thus on the sampling volume.
2. The closest wells to the discharge point give results from the transmissivity distribution that are comparable in mean and variance to the ones obtained from pumping tests because they consider similar support scales.
3. The head data integrate heterogeneities both horizontally and vertically and have a larger support volume than the slug tests, which give the smallest transmissivity estimates. At increasing distance from the outfall, the TF support scales increase. Consequently, both the mean and variability of the estimated transmissivity values increase.

4. This scale effect in transmissivity is due to the nonstationary (maybe fractal) nature of fracture length distributions, which implies that the probability to meet large connected fractures increases with the sampling scale [see also *Le Borgne et al.*, 2006]. Thus, hydraulic head data gives an inexpensive and efficient means to estimate local and global hydraulic transmissivity.
5. For the storage capacity, the scale effect is almost negligible, which indicates that storage is due to vertical connectivity and short horizontal structures as implied by the structural properties of the fractured aquifer.

We then tested the dual-porosity nature of the fractured aquifer by comparing estimates from the single and dual-continuum aquifer models. We found that:

1. The estimates for single-porosity transmissivity and mobile-domain transmissivity were very similar because in the dual-domain model the immobile domain is not transmissive, but merely stores water.
2. The estimates for the storage capacity in the single domain model and the mobile storage capacity in the dual domain model are, as expected, very different.
3. There is a scale dependence in the estimates for the immobile storage capacity which allows determining the characteristic scales of the immobile domain. Thus, the transfer function analysis based on a dual-continuum model allows in principle to extract the distribution of immobile storativity and characteristic spatial scales of the immobile regions.

In conclusion, this analysis shows that the interpretation of hydraulic head data on different scales through frequency analysis using transfer functions is an efficient and inexpensive method for the estimation of hydraulic parameters. More than this, in principle it allows to extract information on the heterogeneity scales and dual-domain nature of the fractured medium.

#### Acknowledgments

XS acknowledges support from the ICREA Academia Project. MD acknowledges the support of the European Research Council (ERC) through the project MHetScale (617511). The authors endorse AGU data policy. All the data and additional information used and cited in this paper can be provided by the corresponding author (DP) at specific requests. The authors acknowledge the useful suggestions provided by three anonymous reviewers, who helped to improve the quality of our manuscript.

#### References

- Barton, C. C., and E. Larsen (1985), Fractal Geometry of Two-Dimensional Fracture Networks at Yucca Mountain, Southwestern Nevada, *Fundamentals of Rock Joints: Proceedings of the International Symposium on Fundamentals of Rock Joints*, pp. 77–84. [Available at <http://core.scholar.libraries.wright.edu/ees/74/>.]
- Bear, J. (1972), *Dynamics of Fluids in Porous Media*, Elsevier, N. Y.
- Beckie, R. (1996), Measurement scale, network sampling scale, and groundwater model parameters, *Water Resour. Res.* 32(1), 65–76, doi:10.1029/95WR02921.
- Berkowitz, B. (2002), Characterizing flow and transport in fractured geological media: A review, *Adv. Water Resour.*, 25(812), 861–884, doi:10.1016/S0309-1708(02)00042-8.
- Bonnet, E., O. Bour, N. E. Odling, P. Davy, I. Main, P. Cowie, and B. Berkowitz (2001), Scaling of fracture systems in geological media, *Rev. Geophys.* 39(3), 347–383, doi:10.1029/1999RG000074.
- Brace, W. F. (1980), Permeability of crystalline and argillaceous rocks, *Int. J. Rock Mech. Min. Sci. Geomech. Abstr.*, 17(5), 241–251, doi:10.1016/0148-9062(80)90807-4.
- Brace, W. F. (1984), Permeability of crystalline rocks: New in situ measurements, *J. Geophys. Res.*, 89(B6), 4327–4330, doi:10.1029/JB089iB06p04327.
- BRGM (1990), Opérations de multiracages en écoulement influencé par pompage pour la détermination des paramètres hydrodynamiques de l'aquifère superficiel du site d'El Cabril (Espagne): Tech. Rept. for ENRESA, Univ. Politècnica de Catalunya, Barcelona, 34 pp.
- Carbonell, J., and J. Carrera (1992), MARIAJ, FORTRAN code for the automatic interpretation of pumping tests. User's guide, Univ. Politècnica de Catalunya, E.T.S.I. Caminos, Barcelona, Spain, 1992.
- Carrera, J., X. Sanchez-Vila, J. Samper, F. Elorza, J. Heredia, J. Carbonell, and C. Bajos (1993), Radioactive waste disposal on a highly heterogeneous fracture medium, 1: Conceptual models of ground-water flow, in *Proceedings of the International Association of Hydrogeologists, XXIVth Congress, Hydrogeology of Hard Rocks*, vol. 1, edited by S. B. Banks and D. Banks, pp. 190–202, Geol. Surv. of Norway, Trondheim.
- Carrera, J., X. Sanchez-Vila, I. Benet, A. Medina, G. Galarza, and J. Guimera (1998), On matrix diffusion: Formulations, solution methods and qualitative effects, *Hydrogeol. J.*, 6, 178–190, doi:10.1007/s100400050143.
- Clauser, C. (1992), Permeability of crystalline rocks, *Eos Trans. AGU*, 73(21), 233–238, doi:10.1029/91EO00190.
- Deere, D. (1963), Technical description of rock cores for engineering purposes, *Rock Mech. Rock Eng.*, 1(1), 16–22.
- Denic-Jukic, V., and D. Jukic (2003), Composite transfer functions for karst aquifers, *J. Hydrol.*, 274(14), 80–94, doi:10.1016/S0022-1694(02)00393-1.
- Dentz, M., A. Cortis, H. Scher, and B. Berkowitz (2004), Time behavior of solute transport in heterogeneous media: Transition from anomalous to normal transport, *Adv. Water Resour.*, 27(2), 155–173.
- Erskine, A. D., and A. Papaioannou (1997), The use of aquifer response rate in the assessment of groundwater resources, *J. Hydrol.*, 202, 373–391.
- Gelhar, L. W. (1974), Stochastic analysis of phreatic aquifers, *Water Resour. Res.*, 10(3), 539–545, doi:10.1029/WR010i003p00539.
- Guimera, J., and J. Carrera (2000), A comparison of hydraulic and transport parameters measured in low-permeability fractured media, *J. Contam. Hydrol.*, 41(34), 261–281, doi:10.1016/S0169-7722(99)00080-7.
- Guimera, J., L. Vives, and J. Carrera (1995), A discussion of scale effects on hydraulic conductivity at a granitic site (El Berrocal, Spain), *Geophys. Res. Lett.* 22(11), 1449–1452, doi:10.1029/95GL01493.
- Gustafson, G., and A. Fransson (2005), The use of the Pareto distribution for fracture transmissivity assessment, *Hydrogeol. J.*, 14(1–2), 15–20, doi:10.1007/s10040-005-0440-y.

- Haggerty, R., and S. Gorelick (1995), Multiple-rate mass transfer for modeling diffusion and surface reactions in media with pore-scale heterogeneity, *Water Resour. Res.*, *31*(10), 2383–2400, doi:10.1029/95WR10583.
- Jimenez-Martinez, J., L. Longuevergne, T. Le Borgne, P. Davy, A. Russian, and O. Bour (2013), Temporal and spatial scaling of hydraulic response to recharge in fractured aquifers: Insights from a frequency domain analysis, *Water Resour. Res.*, *49*, 3007–3023, doi:10.1002/wrcr.20260.
- Lai, J., and L. Ren (2007), Assessing the size dependency of measured hydraulic conductivity using double-ring infiltrometers and numerical simulation, *Soil Sci. Soc. Am. J.*, *71*(6), 1667, doi:10.2136/sssaj2006.0227.
- Le Borgne, T., O. Bour, F. L. Paillet, and J. P. Caudal (2006), Assessment of preferential flow path connectivity and hydraulic properties at single-borehole and cross-borehole scales in a fractured aquifer, *J. Hydrol.*, *328*(12), 347–359, doi:10.1016/j.jhydrol.2005.12.029.
- Liao, Z., K. Osenbrück, and O. A. Cirpka (2014), Non-stationary nonparametric inference of river-to-groundwater travel-time distributions, *J. Hydrol.*, *519*, 3386–3399, doi:10.1016/j.jhydrol.2014.09.084.
- Liu, J., D. Elsworth, and B. H. Brady (1999), Linking stress-dependent effective porosity and hydraulic conductivity fields to RMR, *Int. J. Rock Mech. Min. Sci.*, *36*(5), 581–596, doi:10.1016/S0148-9062(99)00029-7.
- Little, M. A., and J. P. Bloomfield (2010), Robust evidence for random fractal scaling of groundwater levels in unconfined aquifers, *J. Hydrol.*, *393*(34), 362–369, doi:10.1016/j.jhydrol.2010.08.031.
- McKenna, S., L. Meigs, and R. Haggerty (2001), Tracer tests in a fractured dolomite. 3: Double-porosity, multiple-rate mass transfer processes in convergent flow tracer tests, *Water Resour. Res.*, *37*(5), 1143–1154.
- Meier, P., J. Carrera, and X. Sanchez-Vila (1998), An evaluation of Jacob's Method for the interpretation of pumping tests in heterogeneous formations, *Water Resour. Res.*, *34*(5), 1011–1025, doi:10.1029/98WR00008.
- Moench, A. F. (1995), Convergent radial dispersion in a double-porosity aquifer with fracture skin: Analytical solution and application to a field experiment in fractured chalk, *Water Resour. Res.*, *31*(8), 1823–1835, doi:10.1029/95WR01275.
- Molénat, J., P. Davy, C. Gascuelodoux, and P. Durand (1999), Study of three subsurface hydrologic systems based on spectral and cross-spectral analysis of time series, *J. Hydrol.*, *222*(1–4), 152–164, doi:10.1016/S0022-1694(99)00107-9.
- Papadopoulos, S. S., J. D. Bredehoeft, and H. H. Cooper (1973), On the analysis of slug test data, *Water Resour. Res.*, *9*(4), 1087–1089, doi:10.1029/WR009i004p01087.
- Pedretti, D., D. Fernández-García, X. Sanchez-Vila, D. Bolster, and D. A. Benson (2014), Apparent directional mass-transfer capacity coefficients in three-dimensional anisotropic heterogeneous aquifers under radial convergent transport, *Water Resour. Res.*, *50*, 1205–1224, doi:10.1002/2013WR014578.
- Pinault, J.-L., V. Plagnes, L. Aquilina, and M. Bakalowicz (2001), Inverse modeling of the hydrological and the hydrochemical behavior of hydrosystems: Characterization of karst system functioning, *Water Resour. Res.*, *37*(8), 2191–2204, doi:10.1029/2001WR900018.
- Priest, S., and J. Hudson (1976), Discontinuity spacings in rock, *Int. J. Rock Mech. Min. Sci.*, *13*, 135–148.
- Russian, A., M. Dentz, T. Le Borgne, J. Carrera, and J. Jimenez-Martinez (2013), Temporal scaling of groundwater discharge in dual and multicontinuum catchment models, *Water Resour. Res.*, *49*, 8552–8564, doi:10.1002/2013WR014255.
- Sanchez-Vila, X., and J. Carrera (1997), Directional effects on convergent flow tracer tests, *Math. Geol.*, *29*(4), 551–569, doi:10.1007/BF02775086.
- Sanchez-Vila, X., and J. Carrera (2004), On the striking similarity between the moments of breakthrough curves for a heterogeneous medium and a homogeneous medium with a matrix diffusion term, *J. Hydrol.*, *294*(1–3), 164–175, doi:10.1016/j.jhydrol.2003.12.046.
- Sanchez-Vila, X., J. Carrera, and J. P. Girardi (1996), Scale effects in transmissivity, *J. Hydrol.*, *183*(12), 1–22, doi:10.1016/S0022-1694(96)80031-X.
- Sanchez Vila, X., P. M. Meier, and J. Carrera (1999), Pumping tests in heterogeneous aquifers: An analytical study of what can be obtained from their interpretation using Jacob's Method, *Water Resour. Res.*, *35*(4), 943–952, doi:10.1029/1999WR900007.
- Schilling, K. E., and Y.-K. Zhang (2012), Temporal scaling of groundwater level fluctuations near a stream, *Ground Water*, *50*(1), 59–67, doi:10.1111/j.1745-6584.2011.00804.x.
- Schulze-Makuch, D., and P. Malik (2000), The scaling of hydraulic properties in granitic rocks, in *Hydrogeology of Crystalline Rocks*, vol. 34, edited by I. Stober and K. Bucher, pp. 127–138, Water Sci. and Technol. Libr., Springer Netherlands.
- Trincheró, P., X. Sanchez-Vila, and D. Fernández-García (2008), Point-to-point connectivity, an abstract concept or a key issue for risk assessment studies?, *Adv. Water Resour.*, *31*(12), 1742–1753, doi:10.1016/j.advwatres.2008.09.001.
- Trincheró, P., R. Beckie, X. Sanchez-Vila, and C. Nichol (2011), Assessing preferential flow through an unsaturated waste rock pile using spectral analysis, *Water Resour. Res.*, *47*, W07532, doi:10.1029/2010WR010163.
- Tsang, Y. W., C. F. Tsang (1989), Flow channeling in a single fracture as a two-dimensional strongly heterogeneous permeable medium, *Water Resour. Res.*, *25*(9), 2076–2080, doi:10.1029/WR025i009p02076.
- Zech, A., S. Arnold, C. Schneider, and S. Attinger (2015), Estimating parameters of aquifer heterogeneity using pumping tests implications for field applications, *Adv. Water Resour.*, *83*, 137–147, doi:10.1016/j.advwatres.2015.05.021.
- Zhang, Y.-K., and K. Schilling (2004), Temporal scaling of hydraulic head and river base flow and its implication for groundwater recharge, *Water Resour. Res.*, *40*, W03504, doi:10.1029/2003WR002094.
- Zhang, Y.-K., and Z. Li (2005), Temporal scaling of hydraulic head fluctuations: Nonstationary spectral analyses and numerical simulations, *Water Resour. Res.*, *41*, W07031, doi:10.1029/2004WR003797.
- Zhou, H., J. J. Gómez-Hernández, and L. Li (2014), Inverse methods in hydrogeology: Evolution and recent trends, *Adv. Water Resour.*, *63*, 22–37, doi:10.1016/j.advwatres.2013.10.014.
- Zinn, B., and C. F. Harvey (2003), When good statistical models of aquifer heterogeneity go bad: A comparison of flow, dispersion and mass transfer in connected and multivariate Gaussian hydraulic conductivity fields, *Water Resour. Res.*, *39*(3) 1051, doi:10.1029/2001WR001146.